Materials Letters 216 (2018) 73–76

Contents lists available at ScienceDirect

Materials Letters

journal homepage: www.elsevier.com/locate/mlblue

Facile synthesis and hydrazine detection activity of Sb_2S_3 films on indium tin oxide electrode

Wenlong Hou [a,b], Huiyun Guo [a], Jianping Zhang [a,c], Jing Xu [a], Lu Liu [c], Zhiwei Zhang [c], Jingkai Yang [a], Bo Liang [a,*], Haiquan Zhang [a,*]

[a] State Key Laboratory of Metastable Materials Science and Technology, Yanshan University, Qinhuangdao 066004, China
[b] Analysis and Test Center, Hebei Normal University of Science and Technology, Qinhuangdao 066600, China
[c] Chemical Engineering College, Hebei Normal University of Science and Technology, Qinhuangdao 066600, China

ARTICLE INFO

Article history:
Received 23 October 2017
Received in revised form 28 November 2017
Accepted 22 December 2017
Available online 24 December 2017

Keywords:
Antimony sulfide
Thin films
Electrodeposition
Hydrazine

ABSTRACT

Antimony sulfide (Sb_2S_3) films on indium tin oxide (ITO) glass substrates were prepared by electrodeposition method followed with heat-treatment process using a thiol–amine as solvent mixture under ambient conditions. The structure and properties of the Sb_2S_3 films were characterized by XRD, SEM, TEM and electrochemical workstation. The results show Sb_2S_3 films mainly consist of orthorhombic phase with micro-nanorods morphology. Sb_2S_3 films exhibit good electrocatalytic activity towards hydrazine oxidation with a low detection limit of 0.4 μM. The facile synthesis method and excellent sensing properties make the Sb_2S_3 films as a promising candidate for potential application in the field of catalysis and environmental.

1. Introduction

As a member of V–VI binary chalcogenides , Sb_2S_3 with an orthorhombic crystalline structure, is an important semiconductor and highly anisotropic semiconductor. Sb_2S_3 as a typical metal chalcogenides is regarded as a potential material have been applied in various fields such as solar energy conversion [1], photosensors [2], electronic nanodevices [3], photocatalyst [4], lithium ion batteries [5]. The film is the main form for the above application areas. Sb_2S_3 thin films have been prepared using various methods such as: chemical bath deposition [6], spin-coating and heat-treatment [7], vacuum thermal evaporation [8], spray pyrolysis [9], electrodeposition technique [10]. Among them, the electrodeposition in solutions was a cost-effective method for preparing large-area thin films, in terms of its arbitrary substrate shapes, low-temperature processing, and controlling the film thickness. More recently, Brutchey and co-workers describes a simple and general method for the solution processing of bulk V_2VI_3 chalcogenides using a relatively nonhazardous binary solvent mixture [11], which provides a new idea for the study of the structural properties of Sb_2S_3 thin films by solution electrophoresis.

In this letter, we report a facile method to prepare Sb_2S_3 thin films by electrodeposition followed with heat-treatment process on ITO substrate , the resultant Sb_2S_3 thin films shows good electrochemical sensing activity towards hydrazine.

2. Experimental section

1,2-ethanedithiol (edtH2, 97%), 1,2-Ethylenediamine (en, 99%), and Sb_2S_3 (99.9%) were obtained from Aladdin. All reagents were used directly without further purification. Prior to the film deposition, ITO glass substrate with a sheet resistance of 7 $\Omega\,sq^{-1}$ was ultrasonically sequentially cleaned in 2-propanol, acetone, and water each for 15 min, respectively. A two-electrode electrochemical cell was employed consisting of a ITO working electrode and a ITO counter electrode. The electrodeposition was carried out with a stable potential of 4.0 V at room temperature. The durations of the depositions were 0.5 h. The electrolytes were composed of a dilute Sb_2S_3 solution (~0.2 wt%) was filtered using a 0.45 μm filter. The ITO substrate completely turned dark black after electrodeposition indicating that the Sb_2S_3 precursor was deposited on the ITO substrate. The Sb_2S_3 film can be prepared after the precursor was heat-treated under nitrogen to temperatures ranging from 300 °C to 400 °C.

TG (Netzsch STA409 PC), FTIR (Bruker TERSON 27), XRD (Bruker D8 Advance X-ray diffractometer with Ni filtered Cu Kα radiation), SEM (Hitachi S4800), TEM (JEOL-2010) and CHI650E

* Corresponding authors.
E-mail addresses: liangbo@ysu.edu.cn (B. Liang), hqzhang@ysu.edu.cn (H. Zhang).

https://doi.org/10.1016/j.matlet.2017.12.110
0167-577X/

electrochemical workstation (Shanghai Chenhua Company, Shanghai, China) were used to characterize the films. The film on ITO substrate as the working electrode, a platinum wire as counter electrode and saturated Ag/AgCl as the reference electrode. 0.1 M Na_2SO_4 was used as the electrolyte solution. Phosphate buffered saline (PBS, 0.1 M) was prepared by mixing stock solutions of NaH_2PO_4 and Na_2HPO_4.

3. Results and discussion

Fig. 1(a) is TG spectrum of Sb_2S_3 precursor, which was run at the heating rate of 10 °C/min under nitrogen atmosphere and was used to determine the decomposed temperature to prepare Sb_2S_3 film. The TG curves showed that the precursor decompose in two steps at about 80 °C and 200 °C. The first decomposed step of mass loss of 15% may be due to the evaporation of the solvent brought from the electrolytic cell. The second mass loss of about 6% from 200 °C to 300 °C results from the decomposition of the precursor to the Sb_2S_3 micro-nanorods, this may correspond to the dissociation of $[Sb_2S_3]_m[edtH2]_n$ complexes and release of edtH2 through the following reaction (see Eq. (3-1). The negligible mass loss from 300 °C to 400 °C indicated an end-point of decomposition. The decomposition temperature and mass loss of different steps with the literature [19] illustrate the different mechanisms.

$$[Sb_2S_3]_m[edtH2]_n \rightarrow mSb_2S_3 + nedtH2(m:n = 3.64)\uparrow \quad (3\text{-}1)$$

The absorption peaks exhibited by FTIR spectra of en, edtH2 and Sb_2S_3 precursor are as shown in Fig. 1(b). The FTIR spectrum of en shows an absorption peak at 1597 cm^{-1} corresponding to the stretching vibration of N–H bonds. The peak at 1640 cm^{-1} is due to presence of C–H bending vibration in the FTIR spectrum of en, while the peak at 1624 m^{-1} is due to in the FTIR spectrum of edtH2. The bands at 1279 cm^{-1} and 700 cm^{-1} confirm the presence of S–C bonds in edtH2. The band corresponding to–SH group appears at 2560 cm^{-1}. The bands at 1624 cm^{-1}, 1279 cm^{-1} and 700 cm^{-1} of Sb_2S_3 precursor are consistent with $edtH_2$, the band corresponding to the thiol group at 2560 cm^{-1} and the stretching band corresponding to the amino group at 1597 cm^{-1} are not present, which indicating the likely Sb_2S_3 precursor by electrodeposition with concomitant thiolate coordination.

Fig. 2(a) shows the XRD patterns of Sb_2S_3 thin films after heat treatment at 350 °C, which displays the main peak positions of the stibnite mineral (JCPDS No. 42-1393). Apart from the peak of ITO substrate (designated by ◆), no obvious impurity peaks such as oxides or Sb elements are detected in these patterns, suggesting the high purity of the film. EDX spectrum (as shown in Fig. 2(b)) proves that Sb and S exist in this product. Quantitative analysis gives a rough molar ratio Sb:S as nearly 2:3 from the peak area, further proving the purity of film.

Fig. 2(c) and (d) show the FESEM images of Sb_2S_3 micro-nanorods film. It's clearly demonstrated that the films consist of rods with grown along the various directions and the different dimensions. The Sb_2S_3 films deposited on ITO substrate is determined to be ~1.4 μm in thickness from the SEM cross-sectional image. Fig. 2(e) and (f) display TEM and HRTEM images of a Sb_2S_3 nanorod with diameter of 80 nm. The interplanar distance of the fringes is measured to be 0.56 nm which is consistent with the spacing of the (2 0 0) planes for the orthorhombic structure (JCPDS No. 42-1393). It also implies that the nanorod growth direction is along the [0 0 1] direction. The nucleus combine with each other and grow continuously to form nanorods, then small nanorods assimilate into larger nanorods and form extended micro-nanorods through Ostwald ripening, which may be the possible growth mechanism. This can be explained on the basis of a typical Sb_2S_3 crystal structure. It consists of an infinite $(Sb_4S_6)_n$ moiety, parallel to the c-axis, containing two types of Sb and three types of S atoms. Due to the much weaker bonding between these chains than those within the chains, Sb_2S_3 tends to form one-dimensional structures under selected growth conditions, such as nanorods [1,4], nanowires [3,12] and nanoribbons [13].

Fig. 3(a) is the cyclic voltammogram (CV) for bare ITO and Sb_2S_3 films on ITO substrate (Sb_2S_3/ITO) toward the oxidation of hydrazine in the presence of 20 mM hydrazine. It could be seen that both bare ITO and Sb_2S_3/ITO electrodes show a weak electrocatalytic oxidation current toward hydrazine. The oxidation current of Sb_2S_3/ITO electrode on hydrazine is larger than the bare ITO electrode. The curve is similar to the previous report [14].

Fig. 3(b) shows the amperometric current-time curve between concentrations of hydrazine and oxidation current. Inset in Fig. 3 (c) displays the calibration curves, which using the correspondence regression equation as two segments: I (μA) = 0.300029 + 0.00588C (R_2 = 0.9960) and I (μA) = 0.52649 + 0.00298C (R_2 = 0.9954). At the second linear section, the current response (the slope of the calibration curve) decreases, indicating a decrease in sensitivity at higher N_2H_4 concentrations. This phenomenon can be attributed to the increase of hydrazine in the solution, and nitrogen bubbles accumulate on the electrode surface, inhibiting the diffusion of more hydrazine molecules, thus restraining the electrochemical response [15]. The good linear responses of hydrazine are 3–71 μM and 71–501 μM for the two segments, with the experimental detection limit of 0.40 μM (S/N = 3). The limit of detection (LOD) was estimated through the formula LOD = 3δ/S,

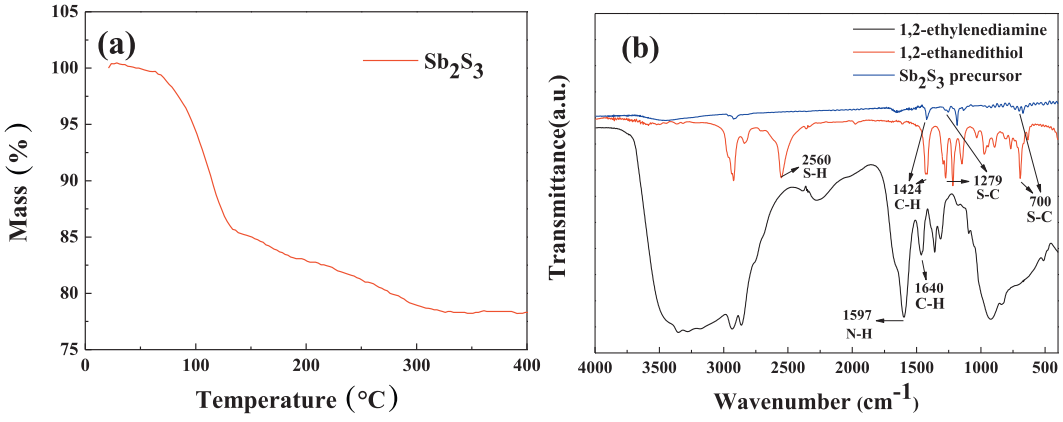

Fig. 1. (a) TG trace of the Sb_2S_3 precursors, (b) FTIR spectra of Sb_2S_3 precursors, 1,2-ethanedithiol and 1,2-Ethylenediamine.